Supporting Information for:

End-to-end azido-pinned interlocking lanthanide squares

Xiao-Lei Li, Jianfeng Wu, Lang Zhao, Wei Shi,* Peng Cheng, and Jinkui Tang*

Experimental Section

General. All starting materials were of A.R. Grade and were used as commercially obtained without further purification. 4, 6-dihydrazinopyrimidine was prepared according to a previously published method.[1]

Elemental analyses for C, H, and N were carried out on a Perkin-Elmer 2400 analyzer. Fourier transform IR (FTIR) spectra were recorded with a Perkin-Elmer FTIR spectrophotometer using the reflectance technique (4000−300 cm^{-1}). Samples were prepared as KBr disks. All magnetization data were recorded on a Quantum Design MPMS-XL7 SQUID magnetometer equipped with a 7 T magnet. The variable-temperature magnetization was measured with an external magnetic field of 1000 Oe in the temperature range of 1.9−300 K. The experimental magnetic susceptibility data are corrected for the diamagnetism estimated from Pascal's tables and sample holder calibration.

Synthesis of the Complex Dy_8L_6

$[Dy_8L_6(\mu_2\text{-}OH)_4(H_2O)_4(N_3)_4(CH_3O)_4]\cdot 16H_2O\cdot 2CH_3OH$ (**Dy_8L_6**).
4,6-dihydrazinopyrimidine (0.1 mmol) was dissolved in a mixture of methanol and acetonitrile (1:3, 20 mL), and then salicylaldehyde (0.2 mmol) was added to the mixture. The reaction mixture was stirred for 30 min. Then, NaN_3 (0.3 mmol) and $Dy(NO_3)_3\cdot 6H_2O$ (0.1 mmol) were added successively. The reaction mixture was stirred at room temperature for 5 h and the resultant solution was left unperturbed to allow for slow evaporation of the solvent. Green single crystals of complex **Dy_8L_6** were obtained after about one week. Yield: 25 mg, (4.9 %, based on the metal salt). Elemental analysis (%) calcd for $C_{114}H_{108}Dy_8N_{48}O_{42}$: C, 33.2, H, 2.6, N, 16.3; found C, 33.5, H, 2.9, N, 16.8.

X-ray Crystallography.

Crystallographic data and refinement details are given in Table S1. Suitable single crystal of **Dy_8L_6** was selected for single-crystal X-ray diffraction analysis. A suitable crystal was selected and on a **'Bruker APEX-II CCD'** diffractometer with graphite monochromated Mo Kα radiation (λ = 0.71073 Å). The crystal was kept at 100(2) K during data collection. The structure was solved by direct methods and refined by the full-matrix least-squares method based on F^2 with anisotropic thermal parameters for all non-hydrogen atoms by using the SHELXS (direct methods) and refined by ShelXL (full matrix least-squares techniques) in the Olex2 package.[1] The locations of Dy and Br atoms were easily determined, and O, N, C atoms were subsequently determined from the difference Fourier maps. Anisotropic thermal parameters were assigned to all non-hydrogen atoms. The H atoms were introduced in calculated positions and refined with a fixed geometry with respect to their carrier atoms. CCDC 1524702 (**Dy_8L_6**) contains the supplementary crystallographic data for this paper. This data can be

obtained free of charge from the Cambridge Crystallographic Data Centre via www.ccdc.cam.ac.uk/data_request/cif.

Table S1. Reported Azido-bridged lanthanides SMMs in the literature.

Complexe	Abbrev.	Bridged groups	Coordination mode/N_3^-	Ueff (K)	Ref.
$[Dy_8L_6(\mu_2\text{-}OH)_4(H_2O)_4(N_3)_4(CH_3O)_4]\cdot16H_2O\cdot2CH_3OH$	**Dy_8L_6**	**-O, N_3**	**end-to-end**	**151.8**	**This work**
$[Dy_4(L1\text{-}2H)_2(L1\text{-}H)_2(N_3)_4(O)]\cdot14H_2O$	Dy_4	-O, -N_3	end-on	51/91	18a
$[Fe_6Dy_3(C_2H_2O_4)(tea)_2(teaH)_4(N_3)_2(N_3)_6(NO_3)]\cdot2EtOH$	Fe_6Dy_3	-O, -N_3	end-on	65.1	18b
$[Cu_2(valpn)_2Tb_2(N_3)_6]\cdot2CH_3OH$	Cu_2Tb_2	-N_3	end-on	30.1	18c
$[Cu_2(valchxn)_2Tb_2(N_3)_6]2CH_3OH$	$[CuTb]_2$	-N_3	end-on	27.6	18i
$[Cr_4Dy_4(OH)_4(N_3)_4(mdea)_4(piv)_4]\cdot3CH_2Cl_2$	$Cr^{III}_4Dy_4$	-OH, -N_3	end-on	15	18d
$[Zn_2Dy_3(m\text{-}salen)_3(N_3)_5(OH)_2]$	Zn_2Dy_3	-OH, -N_3	end-on	13.4	18e
$[Dy_8(bpt)_8(\mu_4\text{-}O)_2(\mu\text{-}OMe)_8(\mu\text{-}_{1,1,3,3}\text{-}N_3)(\mu\text{-}_{1,3}\text{-}N_3)(N_3)_2]\cdot11H_2O\cdot9MeOH$	Dy_8	-NN, -O,-N_3	end-to-end/end-on	9.83	18f
$[Dy_3(N_3)(OH)(H_2L)_3(SCN)_3]\cdot(SCN)\cdot3CH_3OH\cdot H_2O$	Dy_3	-OH, -N_3	end-on	-	18g

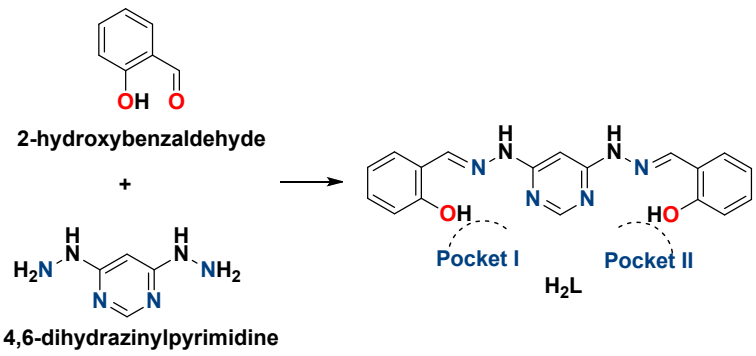

Scheme S1. Structure of the H_2L ligand and two coordination pockets.

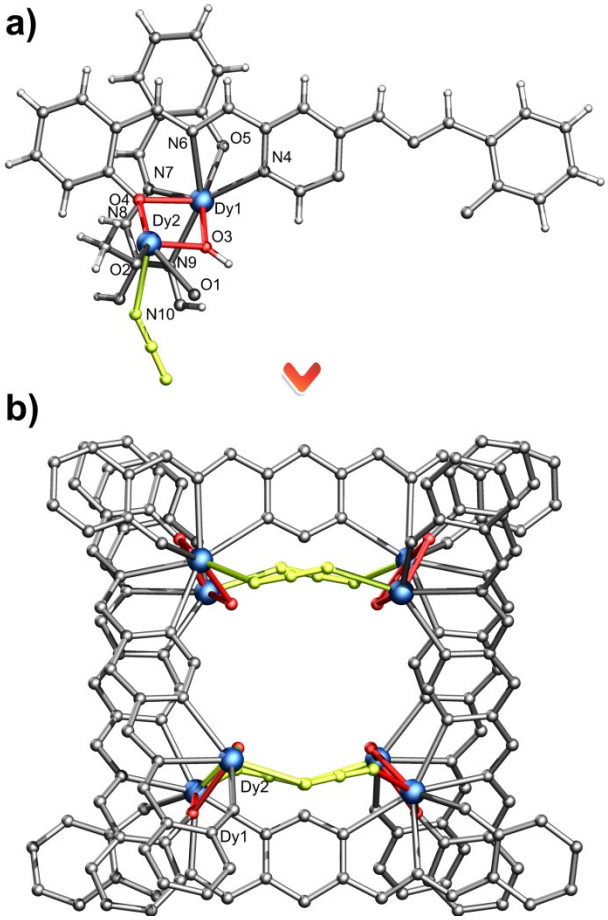

Figure S1. a) Asymmetric unit of the crystal structure of **Dy_8L_6** with atom numbering scheme. b) The crystal structure of **Dy_8L_6**, highlighting the azide (yellow) and μ_2-O (red) bridges, solvent molecules, coordinated methanol and water are not shown for clarity.

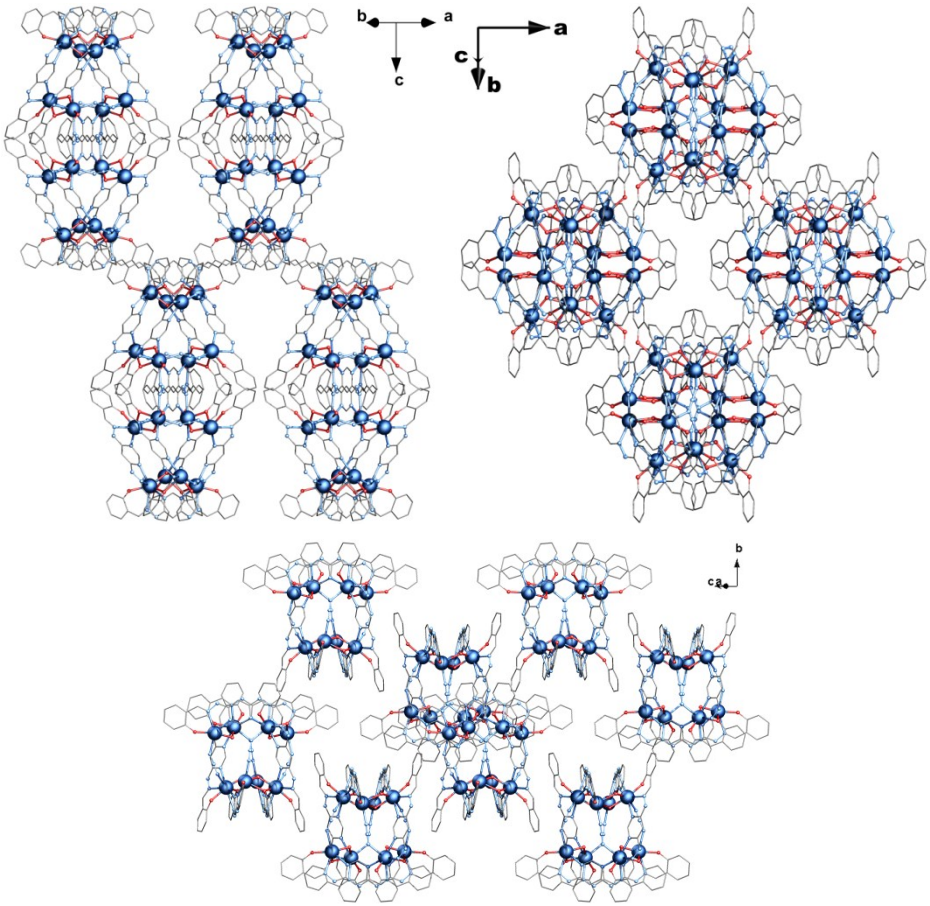

Figure S2. Top) Interesting molecular topologies of **Dy_8L_6** in different crystal packing direction. Bottom) The 3-D topology of the cluster core in giving direction. Solvent molecules, coordinated methanol, water molecules are omitted for clarity.

Table S2. Crystal data and structure refinement for **Dy_8L_6**.

Compound	**Dy_8L_6**
Empirical formula	$C_{114}H_{108}Dy_8N_{48}O_{42}$
Formula weight	4122.48
Temperature/K	100(2)
Crystal system	orthorhombic
Space group	*Fddd*
a/Å	22.7096(10)
b/Å	30.7140(12)
c/Å	52.896(2)
α/°	90
β/°	90
γ/°	90
Volume/Å^3	36895(3)
Z	8
ρ_{calc} g/cm^3	1.484
μ/mm^{-1}	3.272
F(000)	15936.0
Radiation	MoKα (λ = 0.71073)
2 θ range for data collection/°	2.36 to 52.178
Index ranges	-25 ≤ h ≤ 28, -37 ≤ k ≤ 26, -65 ≤ l ≤ 62
Reflections collected	56201
Independent reflections	9142 [R_{int} = 0.0533, R_{sigma} = 0.0369]
Data/restraints/parameters	9141/49/480
Goodness-of-fit on F^2	1.005
Final R indexes [I > = 2σ (I)]	*R_1 = 0.0604, wR_2 = 0.1952
Final R indexes [all data]	*R_1 = 0.0789, wR_2 = 0.2257
CCDC reference code	1524702

*$R_1 = \Sigma||Fo| - |Fc||/\Sigma|Fo|$ for $Fo > 2\sigma(Fo)$; $wR_2 = (\Sigma w(Fo^2 - Fc^2)^2/\Sigma(wFc^2)^2)^{1/2}$ all reflections, $w = 1/[\sigma^2(Fo^2)+(0.1824P)^2 + 60.585P]$ where $P = (Fo^2+2Fc^2)/3$

Table S3. Selected bond lengths for **Dy_8L_6**.

Atom	Atom	Length/Å	Atom	Atom	Length/Å
Dy(2)	Dy(1)	3.7535(6)	N(1)	C(7)	1.274(11)
Dy(2)	O(4)	2.381(6)	N(2)	C(8)	1.353(11)
Dy(2)	O(3)	2.263(6)	N(5)	C(10)	1.339(11)
Dy(2)	O(6)[1]	2.190(6)	N(8)	C(26)	1.337(11)
Dy(2)	O(2)	2.479(8)	N(9)	C(28)	1.323(8)
Dy(2)	O(1)	2.470(10)	N(9)	C(26)	1.356(10)
Dy(2)	N(3)[1]	2.474(7)	N(12)	Dy(1)[2]	2.434(8)
Dy(2)	N(1)[1]	2.558(7)	C(6)	C(1)	1.429(12)
Dy(2)	N(10)	2.431(7)	C(6)	C(7)	1.451(12)
Dy(1)	O(4)	2.303(6)	C(6)	C(5)	1.397(13)
Dy(1)	O(3)	2.242(6)	C(1)	C(2)	1.393(14)
Dy(1)	O(5)	2.262(7)	C(28)	N(9)[2]	1.323(8)
Dy(1)	N(4)	2.526(7)	C(26)	C(27)	1.394(10)
Dy(1)	N(6)	2.567(6)	C(25)	C(24)	1.437(14)
Dy(1)	N(7)	2.553(7)	C(19)	C(24)	1.429(14)
Dy(1)	N(9)	2.526(7)	C(19)	C(20)	1.413(14)
Dy(1)	N(12)[2]	2.434(8)	C(18)	C(13)	1.412(12)
O(4)	C(18)	1.324(10)	C(18)	C(17)	1.410(13)
O(6)	Dy(2)[1]	2.189(6)	C(13)	C(12)	1.445(13)
O(6)	C(1)	1.299(11)	C(13)	C(14)	1.418(12)
O(5)	C(19)	1.320(11)	C(10)	C(9)	1.391(12)
O(2)	C(29)	1.44(3)	C(17)	C(16)	1.387(13)
N(4)	C(10)	1.379(10)	C(9)	C(8)	1.388(12)
N(4)	C(11)	1.291(11)	C(16)	C(15)	1.383(15)
N(6)	N(5)	1.381(10)	C(24)	C(23)	1.409(13)
N(6)	C(12)	1.297(11)	C(23)	C(22)	1.373(16)
N(11)	N(12)	1.165(10)	C(20)	C(21)	1.361(16)
N(11)	N(10)	1.181(10)	C(21)	C(22)	1.41(2)
N(7)	N(8)	1.374(11)	C(2)	C(3)	1.368(14)
N(7)	C(25)	1.272(11)	C(15)	C(14)	1.357(15)
N(3)	Dy(2)[1]	2.474(7)	C(27)	C(26)[2]	1.394(10)
N(3)	C(11)	1.345(11)	C(5)	C(4)	1.356(14)
N(3)	C(8)	1.359(10)	C(4)	C(3)	1.408(15)
N(1)	Dy(2)[1]	2.558(7)	O(8)	C(30)	1.414(18)
N(1)	N(2)	1.385(9)			

[1]1/4-X,+Y,1/4-Z; [2]1/4-X,5/4-Y,+Z

Table S4. Ranges of selected bond angles (°) for **Dy_8L_6**.

Atom	Atom	Atom	Angle/°	Atom	Atom	Atom	Angle/°
O(4)	Dy(2)	Dy(1)	36.02(15)	O(4)	Dy(1)	N(7)	79.5(2)
O(4)	Dy(2)	O(2)	153.0(2)	O(4)	Dy(1)	N(9)	82.8(2)
O(4)	Dy(2)	O(1)	148.1(3)	O(4)	Dy(1)	N(12)[2]	152.3(2)
O(4)	Dy(2)	N(3)[1]	98.5(2)	O(3)	Dy(1)	Dy(2)	33.76(15)
O(4)	Dy(2)	N(1)[1]	78.2(2)	O(4)	Dy(1)	N(7)	79.5(2)
O(4)	Dy(2)	N(10)	102.7(3)	O(4)	Dy(1)	N(9)	82.8(2)
O(3)	Dy(2)	Dy(1)	33.40(14)	O(4)	Dy(1)	N(12)[2]	152.3(2)
O(3)	Dy(2)	O(4)	69.0(2)	O(3)	Dy(1)	Dy(2)	33.76(15)
O(3)	Dy(2)	O(2)	134.6(3)	O(3)	Dy(1)	O(4)	70.8(2)
O(3)	Dy(2)	O(1)	79.1(3)	O(3)	Dy(1)	O(5)	156.3(2)
O(3)	Dy(2)	N(3)[1]	76.9(2)	O(3)	Dy(1)	N(4)	79.6(2)
O(3)	Dy(2)	N(1)[1]	123.3(2)	O(3)	Dy(1)	N(6)	100.9(2)
O(3)	Dy(2)	N(10)	82.8(3)	O(3)	Dy(1)	N(7)	133.7(2)
O(6)[1]	Dy(2)	Dy(1)	118.43(19)	O(3)	Dy(1)	N(9)	78.8(2)
O(6)[1]	Dy(2)	O(4)	84.4(2)	O(3)	Dy(1)	N(12)[2]	89.1(3)
O(6)[1]	Dy(2)	O(3)	143.7(2)	O(5)	Dy(1)	Dy(2)	151.36(15)
O(6)[1]	Dy(2)	O(2)	78.4(3)	O(5)	Dy(1)	O(4)	122.5(2)
O(6)[1]	Dy(2)	O(1)	123.3(3)	O(5)	Dy(1)	N(4)	76.9(2)
O(6)[1]	Dy(2)	N(3)[1]	133.1(2)	O(5)	Dy(1)	N(6)	70.5(2)
O(6)[1]	Dy(2)	N(1)[1]	71.6(2)	O(5)	Dy(1)	N(7)	70.0(2)
O(6)[1]	Dy(2)	N(10)	79.3(2)	O(5)	Dy(1)	N(9)	120.1(2)
O(2)	Dy(2)	Dy(1)	161.4(2)	O(5)	Dy(1)	N(12)[2]	83.3(3)
O(2)	Dy(2)	N(1)[1]	76.7(3)	N(4)	Dy(1)	Dy(2)	93.92(18)
O(1)	Dy(2)	Dy(1)	112.3(2)	N(4)	Dy(1)	N(6)	61.5(2)
O(1)	Dy(2)	O(2)	57.6(3)	N(4)	Dy(1)	N(7)	146.2(2)
O(1)	Dy(2)	N(3)[1]	74.7(3)	N(4)	Dy(1)	N(9)	145.6(2)
O(1)	Dy(2)	N(1)[1]	122.7(3)	N(6)	Dy(1)	Dy(2)	81.22(16)
N(3)[1]	Dy(2)	Dy(1)	83.22(18)	N(7)	Dy(1)	Dy(2)	112.04(19)
N(3)[1]	Dy(2)	O(2)	79.0(3)	N(7)	Dy(1)	N(6)	100.2(2)
N(3)[1]	Dy(2)	N(1)[1]	63.5(2)	N(9)	Dy(1)	Dy(2)	82.53(17)
N(1)[1]	Dy(2)	Dy(1)	100.09(17)	N(9)	Dy(1)	N(6)	149.4(2)
N(10)	Dy(2)	Dy(1)	96.5(2)	N(9)	Dy(1)	N(7)	62.6(2)
N(10)	Dy(2)	O(2)	94.5(3)	N(12)[2]	Dy(1)	Dy(2)	122.0(2)
N(10)	Dy(2)	O(1)	71.3(3)	N(12)[2]	Dy(1)	N(4)	78.7(2)
N(10)	Dy(2)	N(3)[1]	143.0(3)	N(12)[2]	Dy(1)	N(6)	136.0(2)
N(10)	Dy(2)	N(1)[1]	150.7(3)	N(12)[2]	Dy(1)	N(7)	103.2(3)
O(4)	Dy(1)	Dy(2)	37.45(15)	N(12)[2]	Dy(1)	N(9)	74.5(2)
O(4)	Dy(1)	N(4)	114.5(2)	Dy(1)	O(4)	Dy(2)	106.5(2)
O(4)	Dy(1)	N(6)	68.6(2)	Dy(1)	O(3)	Dy(2)	112.8(2)

[1]1/4-X,+Y,1/4-Z; [2]1/4-X,5/4-Y,+Z

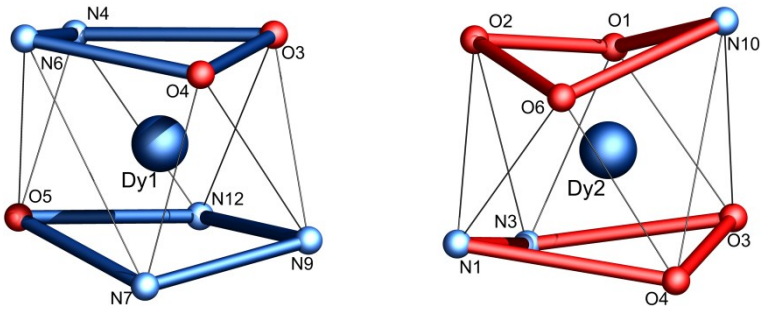

Figure S3. Coordination polyhedra observed in Dy_8L_6: triangular dodecahedron environment for Dy1 and Dy2.

Table S5. Dy^{III} geometry analysis of Dy_8L_6 by SHAPE 2.1 software.[2]

Dy^{III}	TDD-8 (D_{2d})	SAPR-8 (D_{4d})	BTPR-8 (C_{2v})	JBTPR-8 (C_{2v})	JSD-8 (D_{2d})
Dy^{III}(1)	**1.624**	2.691	3.519	4.232	5.357
Dy^{III}(2)	**1.190**	2.713	2.711	3.755	4.128

TDD-8 = Triangular dodecahedron; SAPR-8 = Square antiprism; BTPR-8 = Biaugmented trigonal prism; JBTPR-8 = Biaugmented trigonal prism J50; JSD-8 = Snub diphenoid J84.

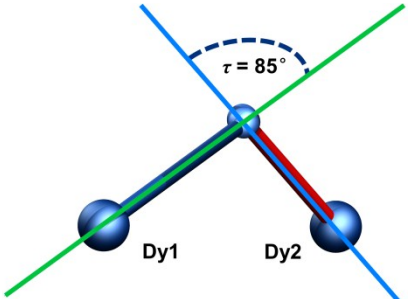

Figure S4. The dihedral angle between the mean planes (blue and green planes) Dy1–N1–N2–N3 and N1–N2–N3–Dy2.

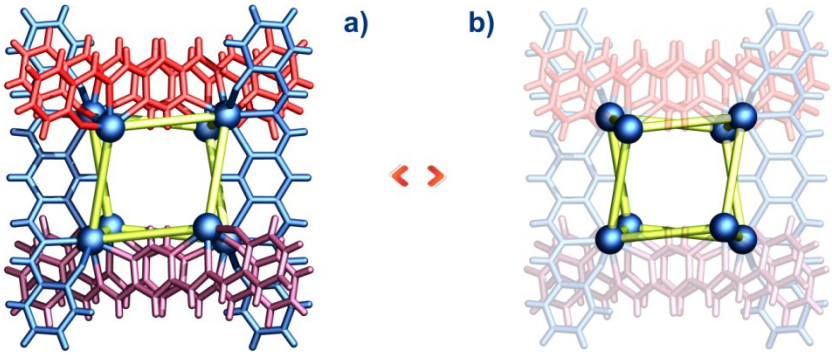

Figure S5. a) Frame-and-sphere representations of crystal structure of **Dy_8L_6**, b) the twisted hexahedron topology is highlighted, solvent molecules, coordinated methanol, water molecules and N_3^- are omitted for clarity.

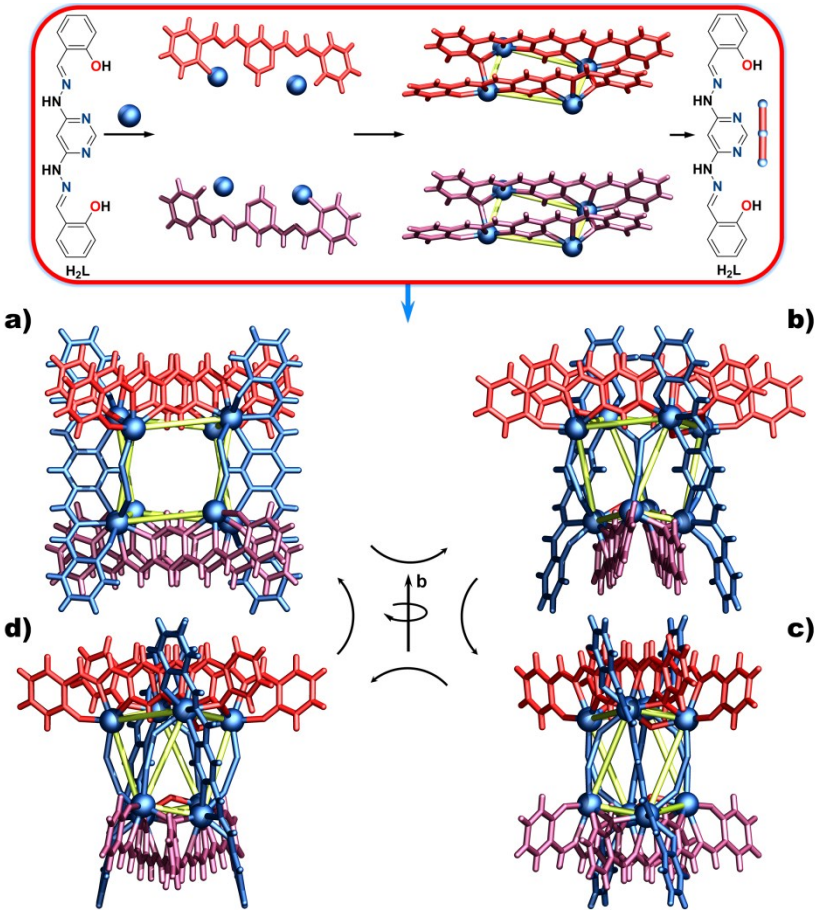

Figure S6. (a-d) Frame-and-sphere representations of self-assembly processes and interesting molecular topologies of **Dy_8L_6** when rotate clockwise from a (a) to c (d) axis along b axis, solvent molecules, coordinated methanol and water molecules are omitted for clarity.

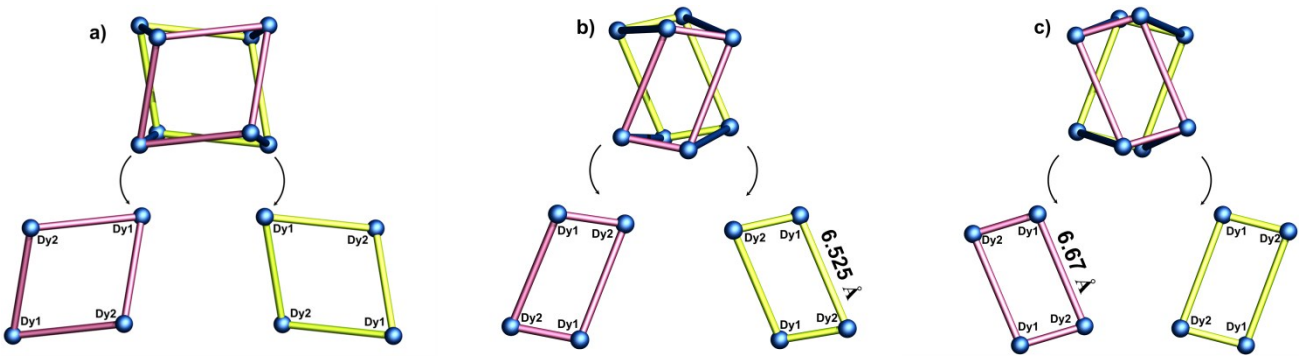

Figure S7. Frame-and-sphere representations of the hexahedron topologies of **Dy_8L_6** along the directions of three faces constructed by the Dy_4.

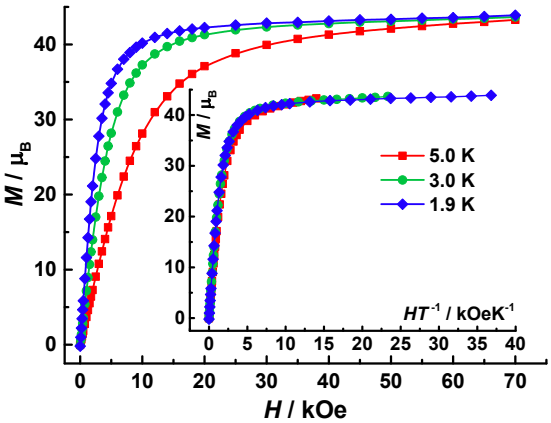

Figure S8. Field dependences of magnetization in the field range 0−70 kOe and temperature range 1.9−5.0 K for **Dy_8L_6**. Inset: Plots of the reduced magnetization *M* versus *H*/*T*.

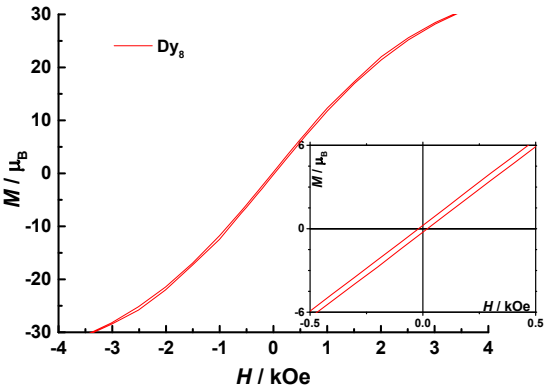

Figure S9. *M* (*H*) hysteresis for **Dy_8L_6** using a scan rate of 2.0 mTs^{-1}.

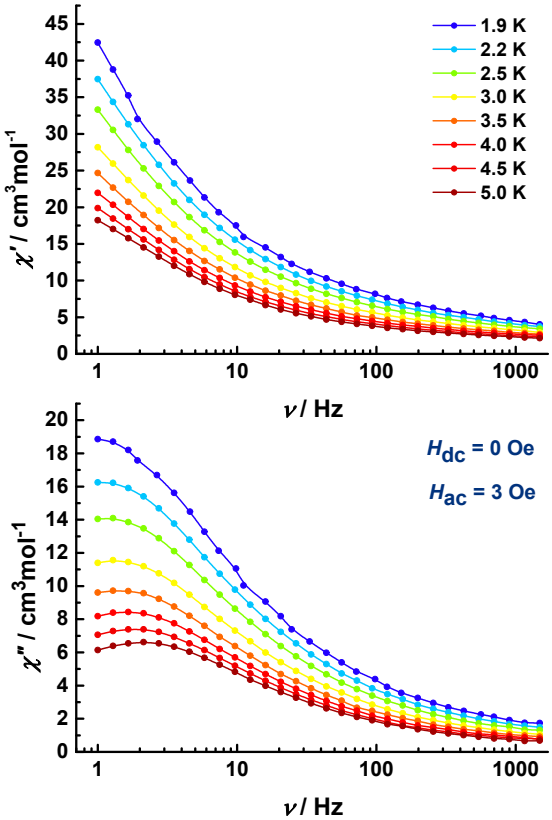

Figure S10. Frequency dependence of the in-phase (χ') and out-of-phase (χ'') ac susceptibility of **Dy_8L_6** between 1.9−5 K in a zero applied dc field. The solid lines are a guide for the eyes.

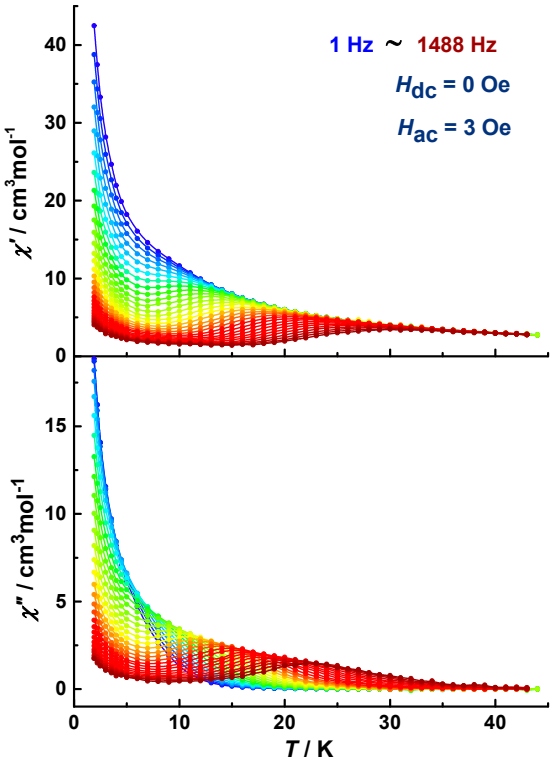

Figure S11. Plots of ac susceptibility *vs*. temperature at H_{ac} = 3.5 Oe, H_{dc} = 0 Oe, oscillating at 1−1488 Hz for **Dy_8L_6** in the temperature range of 2−45 K.

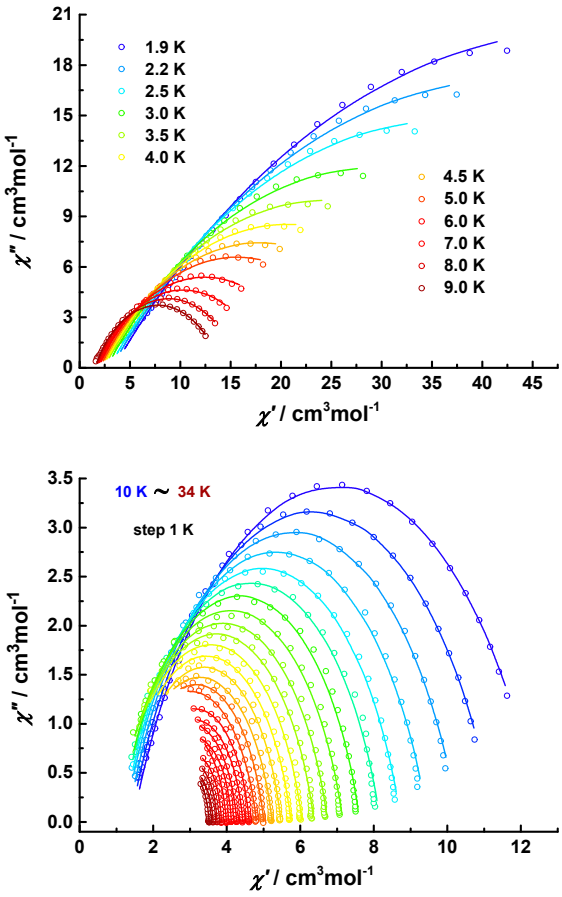

Figure S12. Cole−Cole plots for temperatures between 1.9 and 34 K under a zero dc field with the best fit to the generalized Debye model for **Dy_8L_6**. The Solid lines represent fits to the data, as described in the main text.

Table S6. The best fitting parameters for Cole−Cole plots of **Dy_8L_6** at varying temperatures under zero applied dc field.

T (K)	χ_T	χ_S	α
1.9	0.969267E+02	0.336686E+01	0.486189E+00
2.2	0.821858E+02	0.312776E+01	0.480107E+00
2.5	0.696387E+02	0.291089E+01	0.472493E+00
3.0	0.555834E+02	0.262678E+01	0.462998E+00
3.5	0.459556E+02	0.240224E+01	0.454278E+00
4.0	0.387858E+02	0.226709E+01	0.442876E+00
4.5	0.334321E+02	0.210807E+01	0.435059E+00
5.0	0.292528E+02	0.197617E+01	0.426891E+00
6.0	0.229912E+02	0.182184E+01	0.398809E+00
7.0	0.188394E+02	0.173788E+01	0.366936E+00
8.0	0.160051E+02	0.163618E+01	0.336773E+00
9.0	0.140466E+02	0.153359E+01	0.315098E+00
10.0	0.125177E+02	0.144993E+01	0.293965E+00
11.0	0.112910E+02	0.138211E+01	0.275422E+00
12.0	0.103055E+02	0.130654E+01	0.258565E+00

13.0	0.946975E+01	0.123746E+01	0.247490E+00
14.0	0.873983E+01	0.119965E+01	0.232491E+00
15.0	0.817331E+01	0.113954E+01	0.226107E+00
16.0	0.761951E+01	0.111686E+01	0.213066E+00
17.0	0.715991E+01	0.103861E+01	0.216246E+00
18.0	0.674064E+01	0.105989E+01	0.208357E+00
19.0	0.637227E+01	0.106396E+01	0.200749E+00
20.0	0.604762E+01	0.108861E+01	0.195334E+00
21.0	0.574635E+01	0.116226E+01	0.187992E+00
22.0	0.547074E+01	0.131968E+01	0.170237E+00
23.0	0.523478E+01	0.129723E+01	0.178426E+00
24.0	0.500685E+01	0.133118E+01	0.168420E+00
25.0	0.480524E+01	0.126967E+01	0.176495E+00
26.0	0.460908E+01	0.172584E+01	0.138972E+00
27.0	0.443620E+01	0.190027E+01	0.124616E+00
28.0	0.426921E+01	0.185536E+01	0.120384E+00
29.0	0.412393E+01	0.219494E+01	0.757991E-01
30.0	0.398867E+01	0.180524E+01	0.111912E+00
31.0	0.385271E+01	0.236439E+01	0.517221E-01
32.0	0.373464E+01	0.238866E+01	0.657783E-01
33.0	0.362766E+01	0.246094E+01	0.808166E-01
34.0	0.352111E+01	0.227044E+01	0.939491E-01

$$\ln\tau = -\ln[AT + B + CT^{n} + \tau_0^{-1}\exp(-U_{eff}/k_B T)] \quad (1)$$

	Value	Standard Error
U_{eff}/k_B	151.77487	4.19822
τ	5.83133E-7	7.97465E-8
n	4.5428	0.07201
C	0.0019	3.27296E-4
A	1.38112	0.06245
B	0.76409	0.14625

Table S7. The fitting results and standard errors for the parameters in the Equation 1.

References

1 (a) O. V. Dolomanov, L. J. Bourhis, R. J. Gildea, J. A. K. Howard and H. Puschmann, *J. Appl. Crystallogr.*, 2009, **42**, 339; (b) G. M. Sheldrick, *Acta Crystallogr. A*, 2008, **64**, 112.

2 D. Casanova, M. Llunell, P. Alemany and S. Alvarez, *Chem. Eur. J.*, 2005, **11**, 1479.